Chemico-Biological Interactions 395 (2024) 111006

Contents lists available at ScienceDirect

Chemico-Biological Interactions

journal homepage: www.elsevier.com/locate/chembioint

Research paper

In vitro cleavage of tumor necrosis factor α (TNFα) by Signal-Peptide-Peptidase-like 2b (SPPL2b) resembles mechanistic principles observed in the cellular context

Kinda Sharrouf [a], Christine Schlosser [a], Sandra Mildenberger [a,c], Regina Fluhrer [a,b], Sabine Hoeppner [a,*]

[a] Biochemistry and Molecular Biology, Institute of Theoretical Medicine, Faculty of Medicine, University of Augsburg, Universitätsstrasse 2, D-86159, Augsburg, Germany
[b] University of Augsburg, Center for Interdisciplinary Health Research, 86135, Augsburg, Germany
[c] Institut für Entwicklungsbiologie und Neurobiologie, Johannes Gutenberg-Universität Mainz, Hanns-Dieter-Hüsch-Weg 15, 55099, Mainz, Germany

ARTICLE INFO

Keywords:
Intramembrane aspartyl proteolysis
Signal peptide peptidase family (SPP/SPPL)
In vitro cleavage assay
SPL-707
$(Z\text{-}LL)_2$Ketone
Tumor necrosis factor α

ABSTRACT

Members of the Signal Peptide-Peptidase (SPP) and Signal Peptide-Peptidase-like (SPPL) family are intramembrane aspartyl-proteases like their well-studied homologs, the presenilins, which comprise the catalytically active subunit within the γ-secretase complex. The lack of in vitro cleavage assays for SPPL proteases limited their biochemical characterization as well as substrate identification and validation. So far, SPPL proteases have been analyzed exclusively in intact cells or membranes, restricting mechanistic analysis to co-expression of enzyme and substrate variants colocalizing in the same subcellular compartments. We describe the details of developing an in vitro cleavage assay for SPPL2b and its model substrate TNFα and analyzed the influence of phospholipids, detergent supplements, and cholesterol on the SPPL2b in vitro activity. SPPL2b in vitro activity resembles mechanistic principles that have been observed in a cellular context, such as cleavage sites and consecutive turnover of the TNFα transmembrane domain. The novel in vitro cleavage assay is functional with separately isolated protease and substrate and amenable to a high throughput plate-based readout overcoming previous limitations and providing the basis for studying enzyme kinetics, catalytic activity, substrate recognition, and the characteristics of small molecule inhibitors. As a proof of concept, we present the first biochemical in vitro characterization of the SPPL2a and SPPL2b specific small molecule inhibitor SPL-707.

1. Introduction

Members of the Signal Peptide-Peptidase (SPP) and Signal peptide-Peptidase-like (SPPL) family are intramembrane aspartyl-proteases like their well-studied homologs, the presenilins which comprise the active site of the γ-secretase complex [1]. Intramembrane proteases hydrolyze transmembrane (TM) protein substrates within the hydrophobic core of cellular membranes and by that contribute to membrane protein turnover, and regulation of signaling pathways [2,3]. By altering localization, stability, and function of their target proteins they influence protein-protein interactions [4–7]. Intramembrane cleavage often, but not exclusively, takes place after another protease removes a large part of the substrate protein's extracellular domain (ECD) in a process termed ectodomain shedding [8]. Subsequently, intramembrane proteolysis degrades the remaining membrane-bound substrate fragment and releases an extracellular peptide and an intracellular domain (ICD). This two-step proteolytic process is termed Regulated Intramembrane Proteolysis (RIP) [8].

Presenilins and SPP/SPPL proteases share a core structure of nine TM domains and two conserved active site motifs, a YD-motif in TM domain 6 and a GxGD-motif in TM domain 7, that harbor the catalytically active aspartate residues [9,10]. Since presenilins are involved in the release of the amyloidogenic Aβ-peptide from the amyloid precursor protein (APP), they are critically associated with the development of Alzheimer's disease [11]. The SPP/SPPL family, identified based on sequence similarity to presenilins, in mammals includes five members: SPP, SPPL2a, SPPL2b, SPPL2c, and SPPL3 [3,12–14]. SPP/SPPL proteases are conserved and present in various eukaryotes, including fungi, protozoa, plants, and animals [15]. They are involved in glycosylation of

* Corresponding author. Biochemistry and Molecular Biology, Institute of Theoretical Medicine, Faculty of Medicine, University of Augsburg, Universitätsstrasse 2, Augsburg, D-86159, Germany.
E-mail address: Sabine.hoeppner@med.uni-augsburg.de (S. Hoeppner).

https://doi.org/10.1016/j.cbi.2024.111006
Received 22 December 2023; Received in revised form 27 March 2024; Accepted 14 April 2024
Available online 16 April 2024

Abbreviations

SPP	Signal Peptide Peptidase
SPPL	Signal Peptide Peptidase-like
TNF α	tumor necrosis factor α
NTF	N-terminal fragment
ECD	extracellular domain
ICD	intracellular domain
RIP	Regulated Intramembrane Proteolysis
TM	transmembrane
APP	amyloid precursor protein
ADAM	A Disintegrin and metalloproteinase domain-containing
TACE	Tumor Necrosis Factor α cleaving enzyme
(Z-LL)2-ketone	1,3-di-(Ncarboxybenzoyl-L-leucyl-L-leucyl) amino acetone
IC50	half maximal inhibitory concentration
HRP	horseradish peroxidase
IgG	immunoglobin G
HA	hemagglutinin
dKO	HEK293 cells, that lack endogenous expression of SPPL2a and SPL2b (double knock-out
HEK 293	human embryonic kidney 293
DTT	dithiothreitol
SDS	sodium dodecylsulfate
SDS-PAGE	sodium dodecylsulfate polyacrylamide gel electrophoresis
CHAPSO	3-([3-Cholamidopropyl]dimethylammonio)-2-hydroxy-1-propansulfonat
EDTA	Ethylenedinitrilotetraacetic acid
EGTA	Glycol ether diamine tetraacetic acid
DD/AA	aspartate359alanine, aspartate 421alanine
DMSO	dimethyl sulfoxide
PVDF	polyvinylidene difluoride
TFA	trifluoroacetic acid
MALDI-TOF	Matrix-assisted Laser Desorption/Ionization-Time of Flight
TMB	Tetramethylbenzidine
SEM	standard error of the mean
PC	phosphatidylcholine
PE	phosphatidylethanolamine
CMC	critical micelle concentration

secretory and membrane proteins, vesicular transport, and play roles in physiological and pathophysiological processes such as carcinogenesis, atherosclerosis, immune cell development and function, as well as in the pathogenicity of plasmodia causing Malaria [16]. In vivo, these proteases are localized to different subcellular compartments. While SPPL3 localizes to the medial/early-trans-Golgi apparatus, SPPL2a is mainly found in lysosomes/endosomes, and SPPL2b predominantly localizes to the plasma membrane [17–19]. SPP and SPPL2c are primarily localized to the membrane of the endoplasmic reticulum (ER) [20,21]. Although the physiological function of this protease family slowly begins to emerge, compared to presenilins, only a rather small number of substrates have been identified so far [22]. It is not clear whether this results from a particularly high specificity of these enzymes or whether a lack of appropriate techniques has hampered the discovery of substrates [22]. While it is possible to purify SPP from *E. coli* and recover proteolytic activity in vitro [23], purification of the SPPL proteases or establishment

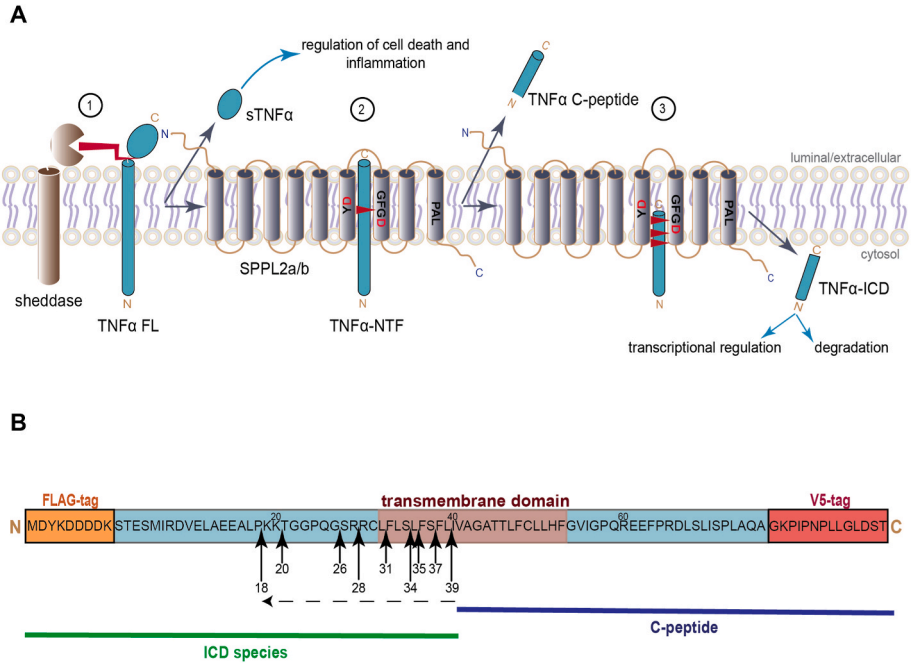

Fig. 1. Schematic representation of TNFα processing: (**A**) RIP of TNFα: The initial cleavage (1) of full-length TNFα (TNFα FL) is catalyzed by a sheddase, such as ADAM10 or ADAM 17 (TACE). This results in release of soluble TNFα (sTNFα) into the lumen/extracellular space, and a membrane spanning N-terminal fragment (TNFα-NTF). Subsequently, TNFα-NTF is cleaved by either SPPL2a or SPPL2b (2) liberating an extracellular peptide (TNFα C-peptide). Multiple consecutive cleavages (3) by SPPL2a or SPPL2b finally release the intracellular domain (TNFα-ICD) to the cytosol. The TNFα-ICD either undergoes degradation or is involved in transcriptional regulation. (**B**) Model substrate for TNFα in vitro cleavage: TNFα-NTF reflects the direct SPPL2a/b in vivo substrate. To allow detection of the products resulting from in vitro cleavage, an N-terminal FLAG-tag and a C-terminal V5-tag were introduced. The TM domain is highlighted in dusky rose an the known SPPL2b cleavage sites (UniProt, P01375 · TNFA_HUMAN) are denoted by arrows. Additionally, the direction of processive SPPL2b cleavage is depicted by a dashed black arrow.

of an in vitro enzymatic assay from independent cell extracts either containing substrate or protease has not been successful so far. Lacking such an in vitro cleavage assay poses several challenges, particularly in the context of understanding substrate selection, enzymatic kinetics, and inhibition by small molecules. But also, a thorough biochemical characterization of these enzymes is not possible as, for instance, high-throughput analyses for substrate and small molecule identification are impaired. This restricts our ability to comprehensively understand substrate specificity and molecular determinants governing enzyme-substrate interactions.

A well-established substrate of SPPL2a and SPPL2b is the N-terminal fragment (NTF) of Tumor Necrosis Factor α (TNFα) that is generated through ectodomain shedding of full-length TNFα by Tumor Necrosis Factor α cleaving enzyme (TACE/ADAM17) and other members of the A Disintegrin and metalloproteinase domain-containing (ADAM) protease family [17,24–26] (Fig. 1A). TNFα-NTF comprises a short ICD plus the TM domain and a short extracellular part up to the TACE cleavage site between alanine 76 and valine 77 [25,27,28]. RIP of TNFα is continued by a SPPL2a or SPPL2b mediated initial cleavage at the C-terminal membrane boundary of the remaining TNFα-NTF, releasing an extracellular peptide (C-peptide) ([26]; Fig. 1A). The shorter, but still membrane bound TNFα-NTF is then further processed by multiple consecutive cleavages [29], finally releasing the ICD to the cytosol, where it is either rapidly degraded or serves as a regulator of Interleukin-12 expression ([17]; Fig. 1A). The characteristic of consecutively removing a TM domain from cellular membranes is termed processivity [30]. While SPPL2b processes TNFα wt only in the context of RIP, SPPL2a was shown to also accept full-length TNFα for direct cleavage in the plane of the membrane, which is termed non-canonical shedding [30].

Contrary to our expectations, established conditions for in vitro γ-secretase cleavage [31–35] did not allow catalytic activity of SPPL2b in vitro. Thus, we stepwise optimized the conditions to specifically allow cleavage of TNFα-NTF by SPPL2b and confirmed that catalytic activity is abolished upon mutation of the catalytic aspartates. Catalytic activity was significantly reduced by the established SPP/SPPL inhibitor $(Z\text{-}LL)_2$-Ketone (1,3-di-(N-carboxybenzoyl-l-leucyl-l-leucyl)amino acetone) [35] and the typical consecutive cleavage [29] of the TNFα TM domain by SPPL2b was also reproduced in vitro. Transferring the assay to a plate-based readout allows fast and high throughput analysis as demonstrated by the first biochemical characterization and in vitro IC50 determination of the SPPL2a/b specific inhibitor SPL-707 [36]. This creates the basis for further higher throughput analysis of enzyme-substrate interaction but also for facilitating drug development by rapid screening of large compound libraries to identify further enzyme inhibitors, activators, and modulators.

2. Theory

Despite many efforts, so far, no consensus sequence or specific structural motif crucial for substrate recognition, cleavage, and processive degradation by SPPL proteases have been identified [3,37] and also the kinetics of substrate recognition and cleavage remain enigmatic. One reason for this is that co-expression of enzyme and substrate in the same cell poses certain obstacles to the thorough analysis of enzyme substrate interaction. These obstacles include the proteins being subject to intracellular regulatory mechanisms as well as to different subcellular localizations, which could result in enzyme and substrate only meeting in a compartment upon yet to be discovered stimuli or signaling events. By developing a cell-independent in vitro cleavage assay for SPPL2b, we aim to overcome these limitations that hamper the identification of novel substrates and the definition of common substrate recognition criteria. In addition, this will allow profound kinetic and biochemical characterization as well as the development of potent and specific small molecule inhibitors and modulators in the future.

3. Materials and methods

3.1. Antibodies

The rabbit polyclonal antibody against FLAG epitopes was purchased from Sigma-Aldrich (ANTI-FLAG® antibody produced in rabbit, F7425, Sigma-Aldrich, Darmstadt, Germany). The rabbit polyclonal antibody against V5 epitopes was purchased from Sigma-Aldrich (*Anti*-V5 Epitope Tag Antibody, AB3792, Sigma-Aldrich, Darmstadt, Germany). The horseradish peroxidase (HRP)-conjugated antibody clone 3F10 against the HA epitope was purchased from Sigma-Aldrich (Darmstadt, Germany). Secondary antibodies, HRP-conjugated goat polyclonal anti-rabbit IgG and anti-mouse IgG antibodies were purchased from Promega (Germany).

3.2. Molecular cloning and cDNA constructs

TNFα-NTF was generated by inserting an N-terminal FLAG-tag (MDYKDDDDK) and a C-terminal V5 tag (GKPIPNPLLGLDST) followed by a stop codon, immediately after amino acid 76 of the full-length protein (Fig. 1B). The cDNA was subcloned into the pcDNA 3.1. Hygro + vector (Invitrogen Life Sciences) utilizing the HindIII and XhoI sites. TNFα-NTF utilized for detection of the C-peptide comprises an N-terminal V5-tag (GKPIPNPLLGLDST) and a C-terminal modified FLAG-tag (DYKDDDDKAP) followed by a stop codon [30]. The cDNA was subcloned into the pcDNA 3.1. Hygro + vector (Invitrogen Life Sciences) utilizing the HindIII and NotI sites. To establish the tagged SPPL2b variants, a C-terminal HA tag (AYPYDVPDYA) followed by a stop codon was C-terminally added to the human cDNA of SPPL2b and SPPL2b D359A, D421A (SPPL2b DD/AA). The resulting cDNAs were subcloned into the EcoRI and XhoI sites of pcDNA4_TO_myc-His A (Invitrogen Life Sciences). All expression constructs were sequence-verified prior to experimental use.

3.3. Cell culture and protein expression

HEK 293 T-Rex cells lacking endogenous SPPL2a and SPPL2b expression (dKO) have been described earlier [30] and were maintained in DMEM GlutaMAX™ medium (Catalog number: 31966047, ThermoFisher, Waltham, USA) supplemented with 10 % (v/v) fetal calf serum (Sigma-Aldrich, St. Louis, USA), 1 % (v/v) penicillin/streptomycin (Life Technologies, New York, USA), 2 μM L-glutamine (Life Technologies Limited, Paisley, UK), and 5 μg/ml Blasticidin (Thermo Fisher Scientific). For TNFα-NTF expression these cells were transiently transfected at 80–90 % confluency with the expression plasmid of TNFα-NTF using Lipofectamine™ 2000 (Invitrogen, Hennigsdorf, Germany) according to the manufacturer's instructions. Cells were then kept in culture for 48 h before harvesting. Protease expression was achieved by stably transfecting dKO cells with either the expression plasmid for SPPL2b wt-HA or that for HA-tagged SPPL2b D359A,D421A (SPPL2b DD/AA-HA). To establish stable cell lines plasmids were transfected using Lipofectamine™ 2000 (Invitrogen, Hennigsdorf, Germany) according to the manufacturer's instructions, followed by selection of single-cell clones in the presence of 200 μg/ml Zeocin (Invitrogen, Hennigsdorf, Germany). Single cell clones were maintained in DMEM GlutaMAX™ supplemented with 10 % (v/v) fetal calf serum, 1 % (v/v) penicillin/streptomycin, 2 μM L-glutamine, 5 μg/ml Blasticidin, and 200 μg/ml Zeocin. Expression of the respective SPPL2b variant was induced at 80–90 % confluency by addition of 1 μg/ml of doxycycline (Sigma Aldrich, Darmstadt, Germany) to an otherwise antibiotic-free culture medium at least 48 h prior to harvesting.

3.4. Cell extracts and solubilized membrane preparations for in vitro assay

Cells from one 10 cm dish were harvested on ice, followed by

centrifugation at 1000 g for 5 min. The resulting pellet was resuspended in 100 μl assay buffer containing 40 mM Tris (pH 7.8), 40 mM potassium acetate, 1.6 mM magnesium acetate, 100 mM sucrose, 5 % (v/v) glycerol, 0.026 % SDS, 1 % (v/v) CHAPSO, 5 mM DTT, and a protease inhibitor mix (1:500) (P1860, Sigma Aldrich, Darmstadt, Germany). Samples were incubated for 1 h on ice, opened by sonication, and incubated on ice for an additional hour. Supernatants obtained from ultracentrifugation at 100,000 g for 30 min were used in the in vitro assay.

Alternatively, cells from one 10 cm dish were harvested on ice and lysed in ice-cold hypotonic buffer (10 mM Tris, 1 mM EDTA, 1 mM EGTA, pH 7.6) supplemented with a protease inhibitor mix (1:500) (P1860, Sigma Aldrich, Darmstadt, Germany) and 5 mM DTT, followed by incubation for 10 min on ice. Cells were mechanically opened (15x needling) using a syringe with a 0.6 mm needle followed by centrifugation at 1000 g for 15 min at 4 °C. The resulting supernatants were centrifuged at 16,000 g for 45 min at 4 °C. The resulting membranes were solubilized in assay buffer and incubated for 1 h on ice, followed by ultracentrifugation at 100,000 g for 30 min at 4 °C. The resulting supernatants were used in the in vitro assay. For membrane solubilization of the TNFα-NTF with an N-terminal V5-tag and a C-terminal modified FLAG-tag, a mixture of ADAM inhibitors (5 μM GI254023X (Sigma-Aldrich) and 10 μM Batimastat (ApexBio, A2577)) as well as general protease inhibitors (Pierce™ Protease Inhibitor (Thermo Scientific, Rockford, USA) and cOmplete™ (Roche, Mannheim, Germany)) were added during the preparation.

3.5. In vitro assay

For each assay condition, 200 μl SPPL2b wt or 700 μl SPPL2b DD/AA preparation were mixed with 50 μl TNFα preparation. 25 μl of pre-equilibrated agarose beads coupled to monoclonal anti-FLAG M2 antibody (ANTI-FLAG® M2 Affinity Gel, Sigma Aldrich, Darmstadt, Germany) were added. Samples were incubated at 37 °C in a rotator (Loopster, IKA, Staufen, Germany) for the indicated time periods. After the respective incubation periods, TNFα-NTF and TNFα-ICDs were pulled down via centrifugation at 3000 g for 3 min at 4 °C. The samples were washed twice with assay buffer containing a reduced CHAPSO concentration (0.5 % CHAPSO) before boiling in SDS-sample buffer for 10 min at 95 °C (or 65 °C for protease expression control samples). For time course experiments, the 0-min time point mixtures were per-incubated for 30 min on ice in a rotator and then immediately centrifuged, washed and boiled in SDS-sample buffer. As indicated in the results section, different concentrations of cholesterol (Sigma-Aldrich, Darmstadt, Germany), L-α-phosphatidylcholine (Sigma-Aldrich, Darmstadt, Germany), SPL-707 [36] (inhibitor (S)-2-cyclopropyl-N1-((S)-5, 11-dioxo-10,11-dihydro-1H,3H,5H-spiro[benzo[d]pyrazolo [1,2-a] [1, 2]diazepine-2,1′-cyclopropan]-10-yl)-N4-(5-fluoro-2-methylpyridin-3-yl)succinimide, MedChemExpress, New Jersey, USA), and $(Z\text{-}LL)_2$-Ketone [35] (Sigma-Aldrich, Darmstadt, Germany) were added to the assay mixture. Inhibitors were added from DMSO stock solutions. The DMSO concentration was adjusted to 1.7 % in every condition. For the detection of the C-peptide the TNFα-NTF with an N-terminal V5-tag and a C-terminal modified FLAG-tag was used as the model substrate and a mixture of ADAM inhibitors (5 μM GI254023X (Sigma-Aldrich) and 10 μM Batimastat (ApexBio, A2577)) as well as general protease inhibitors (Pierce™ Protease Inhibitor (Thermo Scientific, Rockford, USA) and cOmplete™ (Roche, Mannheim, Germany)) were supplemented during the assay incubation.

3.6. SDS–PAGE and immunoblotting

For the separation of TNFα-NTF and TNFα-ICD species, a modified Tris-Tricine gel was used [26]. Proteases were separated on 12 % SDS-PAGE. To detect TNFα-NTF and TNFα-ICD species, gels were blotted on PVDF membranes for 30 min at 400 mA. For TNFα C-peptide detection, gels were blotted on nitrocellulose membranes for 30 min at 400 mA. Regarding SPPL2b protease detection, gels were blotted on PVDF membranes for 1 h at 400 mA. Blocking of non-specific antibody binding was performed using I-Block™ (T2015, Invitrogen I-Block™ protein-based blocking reagent), according to the manufacturer's instructions. Proteins were visualized using Westar Supernova (Cyanagen, Bologna, Italy) or Westar Antares (Cyanagen, Bologna, Italy). For detection of several proteins from the same membranes, especially for detection of a V5-tag following detection of a FLAG-tag, membranes were stripped by incubation in 50 ml stripping buffer (70 mM Tris pH 6.7, 2 % SDS, 7 mM β-mercaptoethanol) for 15 min at 50 °C. Afterwards, membranes were washed repeatedly with TBST, blocked with I-Block™ for 1 h and then incubated with the respective new antibody as described above.

3.7. Mass spectrometry

TNFα in vitro assays were performed as described above. After incubation at 37 °C, remaining TNFα-NTF and the TNFα-ICD species were pulled down by centrifugation at 3000 g for 3 min at 4 °C. Isolated peptides were washed three times with washing buffer (0.14 M NaCl, 0.1 % N-octyleglycopyranoside, 10 mM Tris-HCl pH 7.6, 5 mM EDTA) and two times with dH_2O. Peptides were eluted with 0.3 % TFA and 50 % α-cyano-4-hydroxycinnamic acid matrix in dH_2O (Sigma Aldrich, Darmstadt, Germany). For comparison with TNFα-ICD species derived from co-expression of substrate and enzyme in the same cell, samples were prepared as previously described [30]. Three times 0.4 μL of sample was spotted on an MTP 384 ground steel target plate (Bruker Daltonik GmbH, Germany) and left to dry at room temperature. Masses of the peptides were measured in a rapifleX MALDI Tissuetyper MALDI-TOF/TOF mass spectrometer (Bruker Daltonik GmbH) in a positive linear mode using a mass range of 2000–10000 Da with external calibration.

3.8. Plate-based TNFα in vitro cleavage assay

For equal distribution of magnetic anti-FLAG agarose beads (A36797, Thermofisher) onto a standard flat-bottom 96-well plate, 10 μl of pre-equilibrated beads per well were dissolved in a larger buffer volume corresponding to 200 μl per well and transferred with a multichannel pipette. At each step, beads were allowed to settle for 1 min with the plate locked onto a handheld Magnetic Washer (Millipore) before removing any liquids. The same assay conditions as for the Western Blot-based setup were used but the amounts were scaled down to 50 μl solubilized membranes from SPPL2b expressing dKO cells and 20 μl solubilized membranes from TNFα-NTF expressing dKO cells. To avoid signal loss due to premature cleavage by ADAMs and other proteases, 5 μM GI254023X (Sigma-Aldrich) and 0.02 % azide were added. To minimize pipetting errors, SPL-707 was dissolved in 100 % DMSO at different stock concentrations to allow addition of the same volume to each individual condition. The final DMSO concentration in every condition was 1 %. As blank value, magnetic beads were treated like in all other samples, but instead of solubilized membranes the same volume of assay buffer was applied. Samples were mixed at 100 rpm on a horizontal shaker at 37 °C before removing the supernatant. Beads were washed three times with 200 μl I-Block™ (Invitrogen). At the last washing step, the beads were incubated in I-Block™ (Invitrogen) for 15 min in the presence of 50 μM SPL-707 and 5 μM GI254023X to block ongoing cleavage after the end of the incubation time. *Anti*-V5-HRP-coupled monoclonal antibody (R961-25, Invitrogen) was incubated on the beads in the presence of 50 μM SPL-707 and 5 μM GI254023X for 1 h in I-Block™ (Invitrogen) (dilution 1:3000) at RT while shaking at 100 rpm on a horizontal shaker. Beads were washed three times with 200 μl TBST (Tris-buffered saline with Tween20). 100 μl TMB substrate solution (N301, Thermofisher) were added to each well and incubated for

15 min before adding 100 μl stop solution (N600, Thermofisher). To remove beads, the solutions were transferred to a fresh well with a multi-channel pipette before absorption measurement at 450 nm in a plate reader (Epoch2, Biotek). Standard settings of the instrument corrected raw data for absorption at 635 nm. The absorption of the blank well was subtracted from each experimental absorption value. The value for each inhibitor condition was subsequently calculated relative to the signal of the TNFα-NTF remaining after incubation without inhibitor.

3.9. Statistical analysis

Western Blots were analyzed and quantified using Image Lab software (Bio-Rad). Data analysis was performed using the Python programming language [38]. Data visualization was facilitated using Matplotlib library [39] for creating plots, while NumPy [40] was employed for numerical computations. Additionally, SciPy library [41] was employed for statistical analyses. All data presented were representative of at least three samples derived from independent cell preparations (considered as biologically independent replicates) and - if indicated in the respective figure - varying repetitions from the same preparation (considered as technical replicates). To account for differences in sample loading in SDS-gels, all samples were normalized to the ~25 kDa antibody light chain band. To account for variations in protein input in the independent experiments, results from one experiment are depicted relative to the respective non-treated sample. Statistical comparisons between each group and the non-treated group were performed using the Mann-Whitney *U* test for pairwise comparison, and a significance level of $p < 0.05$ was decided to represent a statistically significant effect. All results are represented as mean ± standard error of the mean (SEM).

4. Results

4.1. In vitro cleavage of TNFα-NTF by SPPL2b

As a model substrate for development of an SPPL2b in vitro cleavage assay we chose TNFα-NTF, comprising residues 2 to 76 of TNFα and, thus, reflecting the main product of TACE-cleaved TNFα [27,42,43] and the direct in vivo substrate of SPPL2b [17,26,29]. For reliable detection of the substrate and its cleavage products an N-terminal FLAG- and a C-terminal V5-tag were added (Fig. 1B). To obtain sufficient substrate, TNFα-NTF was transiently expressed in T-REx™-HEK 293 cells (Invitrogen) lacking endogenous SPPL2a and SPPL2b expression (dKO) [30]. In parallel, C-terminally HA-tagged human SPPL2b was stably expressed under a doxycycline-inducible promoter in dKO cells to serve as enzyme source.

Based on the published in vitro γ-secretase assays [31–35], we isolated membranes from the two independent cell lines, solubilized them in 3-([3-Cholamidopropyl]dimethylammonio)-2-hydroxy-1-propansulfonate (CHAPSO) and co-incubated them in a detergent- and lipid-containing buffer. Despite several attempts at optimization, no enzymatic activity could be detected. We then thoroughly compared the conditions of the published γ-secretase assays [31–34] and of the SPP in vitro assay [23,35,44], as well as buffer conditions for solubilization of other membrane proteins [45,46] and came up with a new starting assay condition comprising 40 mM Tris, pH 7.8, 40 mM potassium acetate, 1.6 mM magnesium acetate, 100 mM sucrose, 1 % CHAPSO, 5 % glycerol, 0.025 % SDS, 5 mM DTT, and protease inhibitor mix P1860. To increase the product-signal, substrate and product were immunoprecipitated via the FLAG-tag during proteolysis. In contrast to the established γ-secretase assays that are carried out in the presence of the membrane solubilizing detergent CHAPSO below its critical micelle concentration (CMC) at 0.1–0.25 %, these assay conditions resemble a CHAPSO concentration above the CMC.

Cells expressing TNFα-NTF and cells expressing SPPL2b were separately lysed in hypotonic buffer, and membranes were isolated prior to solubilization. Alternatively, cells were separately lysed by sonication directly in the assay buffer. Both strategies revealed equivalent results. Solubilized membranes or lysates were cleared by ultracentrifugation before combining substrate and protease or, as negative control, the same amount of cleared lysate from dKO cells. The mixtures for the 0-min time points were kept on ice for 30 min on the rotator wheel during immunoprecipitation and subsequently washed before addition of SDS-sample buffer. All other samples were incubated at 37 °C in the rotator for the indicated periods. (Fig. 2A). Substrate and the N-terminal cleavage products (TNFα-ICD species) were visualized by Western Blot with a polyclonal anti-FLAG antibody following SDS-PAGE (Fig. 2A). TNFα-NTF appears in multiple bands that slightly differ in molecular weight (Fig. 2A). Since these TNFα-NTF species all comprise the N-terminal FLAG-tag and are also detected in control samples, which do not contain catalytically active SPPL2b, they most likely originate from C-terminal trimming by an unrelated protease. This is supported by the visualization of the same samples with an *anti*-V5 antibody that results in detection of a single TNFα-NTF band (Fig. 2B).

Compared to the respective control sample, already after 30 min incubation time of TNFα-NTF with catalytically active SPPL2b, generation of TNFα-ICD and reduction of the substrate were detected (Fig. 2A). As observed previously upon incubation of membranes from cells co-expressing substrate and protease [29,30], after prolonged incubation time increasing amounts of smaller TNFα-ICD species were detected (Fig. 2A), indicating that processive substrate cleavage also takes place in an in vitro assay that combines SPPL2b and TNFα-NTF expressed in different cells. Due to this consecutive turnover, TNFα-ICD species are gradually degraded. In addition, over time protein aggregation was observed (Suppl. Fig. 1). Taking the best possible reduction of the substrate and its lowest possible aggregation as a basis, the optimal incubation time is 120 min.

4.2. Impact of membrane lipids on SPPL2b in vitro activity

The in vitro activity of γ-secretase depends on the lipid composition of the assay buffer. In particular, the concentration of phosphatidylcholine (PC) greatly influences the activity of the enzyme in vitro [31]. Therefore, we addressed the importance of the lipid concentration for SPPL2b activity by systematically titrating PC from 0 to 2.5 mg/ml and incubating the samples for 120 min at 37 °C (Fig. 2C, Suppl. Fig. 2A). Since TNFα-ICD species are gradually turned over during incubation, the reduction of TNFα-NTF was used to quantify the enzymatic activity. To ensure that TNFα-NTF reduction is not solely based on variations in sample loading, or the amount of anti-FLAG coupled agarose beads used for immunoprecipitation, the anti-FLAG antibody signal of the ~25 kDa antibody light chain was used for normalization. In contrast to γ-secretase, the PC concentration did not significantly influence the catalytic activity of SPPL2b in vitro. However, we did observe a non-significant tendency for the optimal concentration at 1.5 mg/ml (Fig. 2C, Suppl. Fig. 2A) and chose to perform further experiments at this PC concentration.

4.3. Impact of cholesterol on SPPL2b in vitro activity

Cholesterol has been shown to be an important determinant for the efficiency of intramembrane proteolysis in vivo and in vitro [31,47–49]. To evaluate the importance of cholesterol for SPPL2b in vitro activity we titrated the cholesterol concentration from 0 to 0.25 % (w/v) at 1.5 mg/ml PC for 120 min at 37 °C. As the detergent concentration in the SPPL2b in vitro assay is above the CMC, cholesterol was dissolved directly in the assay buffer to avoid the negative effects of chloroform and methanol solubilization reported for the in vitro γ-secretase assay [31]. At 0.025 % and 0.05 % cholesterol, a statistically significant improvement of SPPL2b activity was observed, with the optimum at 0.05 % cholesterol (Fig. 2D, Suppl. Fig. 2B). Increasing amounts of cholesterol hampered SPPL2b catalytic activity, and cholesterol

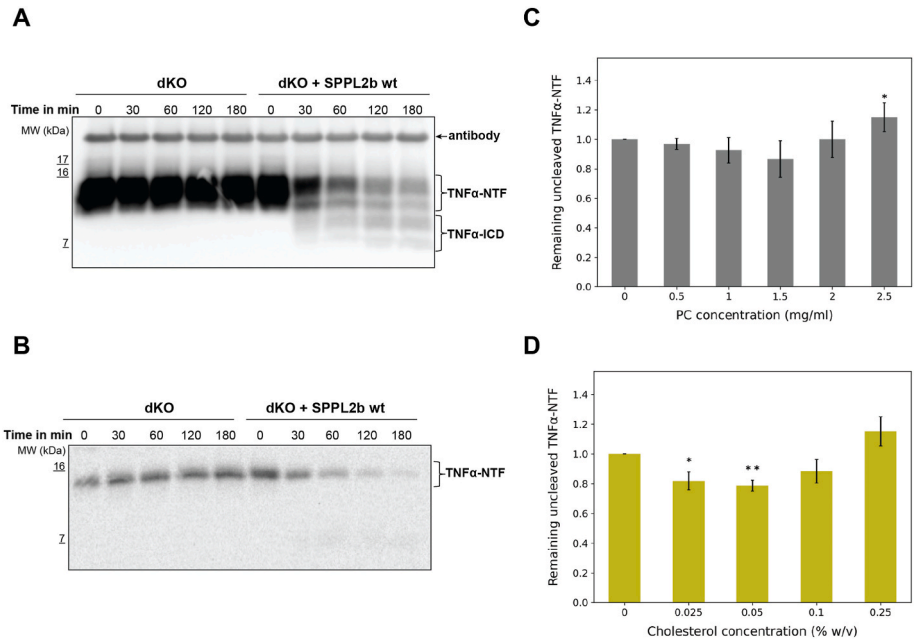

Fig. 2. In vitro cleavage of TNFα-NTF by SPPL2b and assay optimization. Solubilized membranes from HEK293 dKO cells either stably expressing catalytically active SPPL2b (SPPL2b wt) or TNFα-NTF were incubated at 37 °C for the indicated time periods. Solubilized membranes from HEK293 cells lacking endogenous SPPL2a and SPPL2b served as negative control (dKO). (**A**) In vitro cleavage of TNFα-NTF was monitored on Western Blot utilizing the N-terminal FLAG-tag. Over time, TNFα-NTF is reduced, and the resulting TNFα-ICD species are consecutively turned over in the presence of catalytically active SPPL2b. Cross-reaction of the monoclonal anti-FLAG antibody attached to the agarose beads with the polyclonal anti-FLAG antibody used for detection in Western Blot was observed (antibody). (**B**) In vitro cleavage of TNFα-NTF on the same Western Blot as shown in (A) was monitored utilizing the C-terminal V5-tag. (**C**) Impact of phosphatidylcholine (PC) on SPPL2b mediated in vitro TNF*α*-NTF proteolysis: Samples as in (A) were incubated at 37 °C for 120 min in presence of the indicated PC concentrations. The remaining TNFα-NTF was normalized to the antibody signal and quantified relative to the amount of TNFα-NTF remaining after incubation without PC. n = 5 for 0–2 mg/ml PC and n = 4 for 2.5 mg/ml PC (see also Suppl. Fig. 2A). At 2.5 mg/ml PC protein aggregation was frequently observed. Mean ± SEM, Mann-Whitney *U* test for pairwise comparison between each of the groups and the control group without PC (0). *, $p < 0.05$; **, $p < 0.01$. (**D**) Impact of cholesterol on SPPL2b mediated in vitro TNF*α*-NTF proteolysis: Samples were incubated as in (C) in the presence of 1.5 mg/ml PC and the indicated cholesterol concentrations. Quantification was carried out as in (C). n = 7 for 0–0.1 % (w/v) cholesterol and n = 3 for 0.25 % (w/v) cholesterol (see also Suppl. Fig. 2B). At 0.25 % cholesterol, protein aggregation was frequently observed. Mean ± SEM, Mann-Whitney *U* test for pairwise comparison between each of the groups and the control group without cholesterol (0). *, $p < 0.05$; **, $p < 0.01$. Note that reduction of the remaining TNFα-NTF in (C) and (D) indicates increased protease activity.

concentrations above 0.1 % frequently induced aggregation consistent with previously reported observations for the γ-secretase in vitro assay [31].

4.4. TNFα-NTF in vitro cleavage is abolished by catalytically inactive SPPL2b

After determining the optimal lipid composition for SPPL2b in vitro activity, we next verified that turnover of TNFα-NTF is not only based on the presence of SPPL2b but also requires its catalytic activity. To this end, an SPPL2b variant with mutation of both catalytic aspartyl residues, SPPL2b D359A/D421A (SPPL2b DD/AA), was stably expressed in dKO cells under a doxycycline inducible promoter. The in vitro assay was carried out in the presence of similar amounts of either catalytically active SPPL2b or the inactive variant at the optimized lipid composition (Fig. 3A). As expected, reduction of TNFα-NTF as well as production of TNFα-ICD was completely abolished in the presence of SPPL2b DD/AA (Fig. 3B), demonstrating that the observed in vitro activity is based on the catalytic activity of SPPL2b.

As an additional control for our assay and to completely monitor the processing of TNFα-NTF by SPPL2b, we aimed to also detect the TNFα C-peptide that reflects the C-terminal counterpart of the TNFα-ICD and is released after the initial SPPL2b cleavage ([26,30] and Fig. 1). To achieve this, a distinct model substrate had to be employed, comprising TNFα-NTF tagged with an N-terminal V5-tag and a C-terminal FLAG-tag with an alanine-proline addition to avoid degradation of the C-peptide by carboxypeptidases. This would allow us to pull down the C-terminal reaction product via the FLAG-tag but keep the general set-up of our assay. To abolish background signals frequently observed in the negative control, a combination of general protease inhibitors (Pierce™ Protease Inhibitor and cOmplete™) as well as 10 μM of matrix-metalloprotease inhibitor Batimastat, and 5 μM of ADAM10 specific inhibitor GI254023X, were added during every step of the preparation and freezing was avoided throughout the procedure. This almost completely abolished non-SPPL2b related cleavage in the luminal juxtamembrane domain of the substrate. The in vitro cleavage of TNFα-NTF by SPPL2b was conducted under optimized assay conditions and revealed the generation of the TNFα C-peptide in the presence of catalytically active SPPL2b but not in its absence (Fig. 3C). This further supports that cleavage of TNFα by SPPL2b in the newly developed in vitro cleavage assay basically follows the same principles as the processing observed earlier in a cellular context [26,29,30].

4.5. In vitro cleavage site of TNFα-NTF

To further corroborate that the established in vitro conditions resemble the cleavage of TNFα catalyzed by SPPL2b in intact cells, we determined the in vitro cleavage sites using MALDI-TOF mass spectrometry. To this end, either TNFα-ICD species resulting from in vitro cleavage under optimized assay conditions or, as described earlier, those from incubation of membranes co-expressing substrate and enzyme [26,29,30], were isolated utilizing the N-terminal FLAG-tag. Mass spectrometric analysis revealed in vitro cleavage products that qualitatively match those from co-expression setups and are assigned to the known SPPL2b cleavage sites at L39, S34, L35 of the TNFα TM domain and R28 (Fig. 4). In vitro incubation of extracts from cells dKO cells with

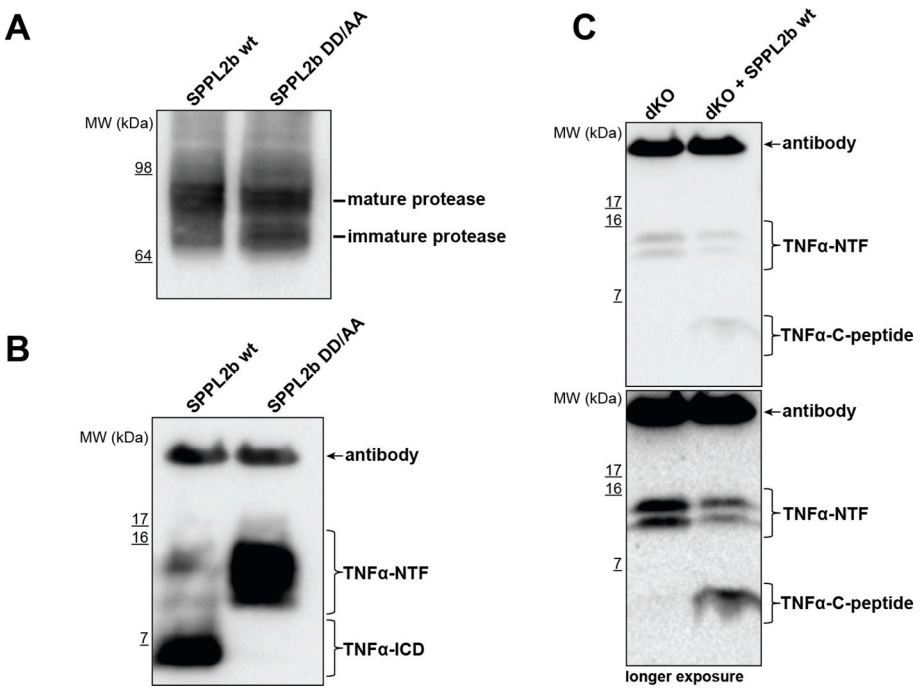

Fig. 3. In vitro cleavage of TNFα-NTF depends on the SPPL2b catalytic activity and reveals TNFα C-peptide. (**A**) TNFα-NTF in vitro cleavage was carried out from membrane preparations at optimized assay conditions as described in Fig. 2 in the presence of similar amounts of either catalytically active SPPL2b (SPPL2b wt) or catalytically inactive SPPL2b (SPPL2b DD/AA). (**B**) In vitro cleavage of TNFα-NTF from the same samples as in (A) was monitored on Western Blot utilizing the N-terminal FLAG-tag. Note that TNFα-NTF is not processed in the presence of SPPL2b DD/AA and TNFα-ICD is only detected in the presence of catalytically active SPPL2b. (**C**) In vitro generation of TNFα C-Peptide by SPPL2b. Solubilized membranes from HEK293 dKO cells either stably expressing catalytically active SPPL2b (SPPL2b wt) or TNFα-NTF with an N-terminal V5-tag and a C-terminal modified FLAG-tag were incubated at 37 °C for 120 min at the optimized assay conditions in the presence of ADAM inhibitors (5 μM GI254023X and 10 μM Batimastat) as well as general protease inhibitors (Pierce™ and cOmplete™). Solubilized membranes from HEK293 cells lacking endogenous SPPL2a and SPPL2b served as negative control (dKO). In vitro cleavage of TNFα-NTF was monitored on Western Blot utilizing the C-terminal FLAG-tag. The presence of catalytically active SPPL2b resulted in generation of TNFα C-peptide.

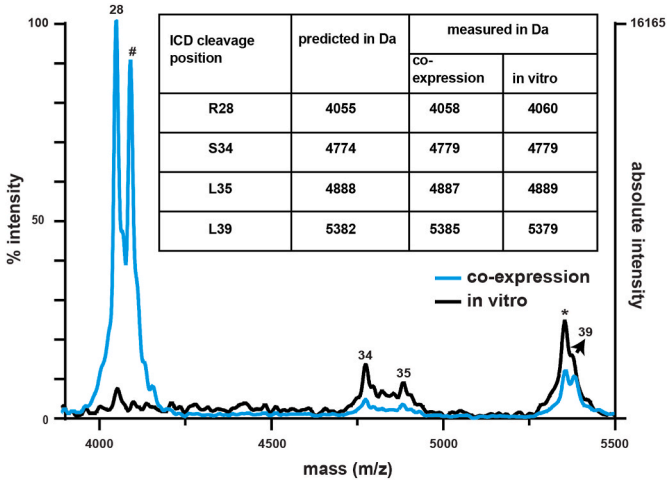

ICD cleavage position	predicted in Da	measured in Da	
		co-expression	in vitro
R28	4055	4058	4060
S34	4774	4779	4779
L35	4888	4887	4889
L39	5382	5385	5379

Fig. 4. In vitro cleavage of TNFα-NTF by SPPL2b reveals the same cleavage sites as observed in a cellular context. TNFα ICD species resulting either from in vitro cleavage carried out at the optimized conditions described in Fig. 2 (black line) and from incubation of intact cell membranes co-expressing substrate and enzyme as described earlier [29,30](blue line) were isolated utilizing the N-terminal FLAG-tag and were analyzed via MALDI-TOF mass spectrometry. Single letter code and numbers indicate position of the most N-terminal amino acid of the respective cleavage product. * marks non-specific background peak, # marks modification of a cleavage product. The Table indicates the experimentally determined masses.

TNFα-NTF served as negative control and revealed unrelated background signals (Suppl. Fig. 3). Interestingly, the major intramembranous cleavages of SPPL2b at L39 and S34 of the TNFα TM domain are more prominently visible in vitro compared to the co-expression setup (Fig. 4). Since substrate and enzyme in the co-expression setup already bind in the living cell and thus, the total time of interaction is longer compared to the in vitro setup, this further supports the consecutive turnover of TNFα by SPPL2b. Moreover, these data confirm that SPPL2b applies the same consecutive cleavage mechanism in vitro as in intact cell membranes.

4.6. *Inhibition of SPPL2b in vitro activity*

Finally, we asked whether the well-established SPP/SPPL inhibitors $(Z\text{-}LL)_2$-Ketone [35] and SPL-707 [36] inhibit SPPL2b activity in vitro, similar to what has been observed earlier. While $(Z\text{-}LL)_2$-ketone is described as a potent inhibitor of SPP and only targets SPPL2b efficiently at higher concentrations [15,35,50], SPL-707 is a specific SPPL2a inhibitor that also inhibits SPPL2b in a low μM range at 0.47 μM [36]. Due to the lack of an in vitro assay, $(Z\text{-}LL)_2$-Ketone for example had been characterized by monitoring the cleavage product from cells co-expressing substrate and protease [51]. SPL-707 had only been tested on SPP, SPPL2a and SPPL2b in animal models or cellular assays using either a luciferase reporter gene or a cellular nuclear translocation imaging assay (high content assay, HCA) [36,52]. To test the potency of these inhibitors in the in vitro assay, catalytically active SPPL2b and TNFα-NTF were incubated for 120 min at the established assay conditions in the presence of increasing inhibitor concentrations (Fig. 5). SPPL2b activity was determined by quantification of the TNFα-NTF reduction relative to a non-treated control (Fig. 5A&B; Suppl. Fig. 4 A &B). Both inhibitors significantly reduced SPPL2b activity already at the

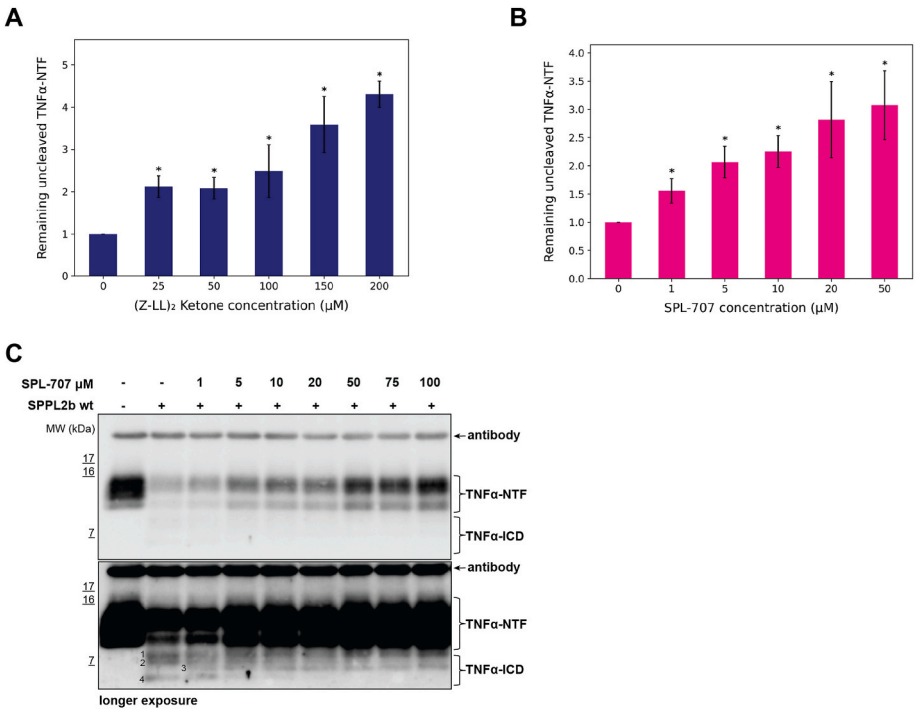

Fig. 5. In vitro cleavage of TNFα-NTF by SPPL2b is inhibited by known SPP/SPPL protease inhibitors. TNFα-NTF in vitro cleavage was carried out at the optimized conditions determined in Fig. 2 in the presence of the indicated inhibitor concentrations. (**A**) Inhibition of SPPL2b by $(Z\text{-}LL)_2$-Ketone (n = 3) and (**B**) inhibition of SPPL2b by SPL-707 (n = 4). The remaining TNFα-NTF was normalized to the antibody signal and quantified relative to the amount of TNFα-NTF remaining after incubation without inhibitor. Note that increase of the remaining TNFα-NTF corresponds to increased inhibition of the protease activity. Mean ± SEM, Mann-Whitney *U* test for pairwise comparison between each of the groups and the control group without Inhibitor (0 μM). *, $p < 0.05$ relative to the respective samples without inhibitor. Representative Western Blots of (A) and (B) are shown in Suppl. Fig. 4. (**C**) Turnover of TNFα-NTF and generation of different TNFα-ICD species (ICD_1 – ICD_4) in presence of the indicated SPL-707 concentrations was monitored in Western Blot utilizing the N-terminal FLAG-tag of TNFα-NTF. Note that with increasing inhibitor concentrations not only TNFα-NTF degradation but also the generation of ICD_4 is reduced while larger ICD species (ICD_1 and ICD_3) accumulate.

lowest concentration tested, as indicated by an increased amount of remaining TNFα-NTF (Fig. 5A&B). As expected from IC_{50} determinations in substrate-enzyme co-expression setups [36,51], much higher concentrations of $(Z\text{-}LL)_2$-Ketone than of SPL-707 were required to achieve a similar relative inhibition of the enzymatic activity (Fig. 5A&B). With increasing inhibitor concentrations, the amount of remaining TNFα-NTF gradually increased, demonstrating concentration dependent effects of these inhibitors on SPPL2b also in vitro (Fig. 5A&B). Reduced degradation of TNFα-NTF induced by increasing SPL-707 concentrations was also observed in Western Blot (Fig. 5C; Suppl. Fig. 4B). In addition, gradual reduction of the smallest TNFα-ICD species (TNFα-ICD_4) and stepwise accumulation of larger TNFα-ICD species (TNFα-ICD_1 and TNFα-ICD_2) was observed (Fig. 5C). This finally corroborates that SPPL2b also in vitro applies consecutive cleavages to the TNFα TM domain as has been observed earlier in intact membranes from cells co-expressing SPPL2b and TNFα [29,30]. Moreover, since the inhibitor not only inhibits generation of the smallest TNFα-ICD species but also induces accumulation of the larger intermediates, this further supports that SPPL2b itself and not any unrelated protease is responsible for this consecutive turnover.

4.7. High-throughput read-out

To facilitate future studies on substrate specificity and kinetics of SPPL2b as well as identification of small molecules inhibiting or activating the enzyme, we aimed to transfer the SPPL2b in vitro assay to a small-scale plate-based format. As commercially available anti-FLAG ELISA plates were not compatible with detergent present in the in vitro assay, anti-FLAG antibodies immobilized on magnetic beads were subjected to a regular 96-well plate and incubated with the assay mix while shaking. This allowed reduction of the total assay volume to 25 % of the volume required in the Western Blot based setup and, thus, substantially reduced the amount of required material. Solubilized membrane preparations of dKO cells transiently expressing TNFα-NTF and of dKO cells stably expressing catalytically active SPPL2b were incubated for 120 min at 37 °C in optimized assay conditions. Solubilized membranes from dKO cells served as negative control. 0.02 % azide and 5 μM GI254023X were added to avoid signal reduction due to bacterial degradation and ADAM-mediated cleavage, respectively. ADAM protease inhibitor was applied since in contrast to the Western Blot, read-out, where the reduction of the TNFα-NTF can still be measured even if the V5 tag is removed by ADAM proteases, loss of the V5-tag during incubation in the plate-based read-out influences activity measurement. To remove the V5-tagged TNFα C-Peptide liberated by the initial SPPL2b cleavage, after incubation, the magnetic beads were carefully washed with I-Block™ utilizing a multichannel pipette, and supernatants of each step were removed during immobilization of the beads on a magnetic plate. Subsequently, the non-cleaved TNFα-NTF was detected in a sandwich ELISA via the C-terminal V5-tag using an HRP-coupled *anti*-V5-antibody to avoid cross reaction between the secondary antibody and the anti-FLAG antibody coupled to the magnetic beads. Thus, also in the plate-based read-out, a higher signal corresponds to lower enzymatic activity. Inhibition of SPPL2b activity with increasing concentrations of SPL-707 revealed similar results (Fig. 6) as the respective Western Blot based assay (Fig. 5B) and these data suggest that the IC50 with 50 % inhibition of biochemical activity [53] is similar to that determined in the cellular HCA screen [36]. This demonstrates that the newly developed in vitro assay can be carried out in a high through put set up, which is amenable to future mechanistic studies of SPPL2b and the development of potent inhibitors and activators of this enzyme.

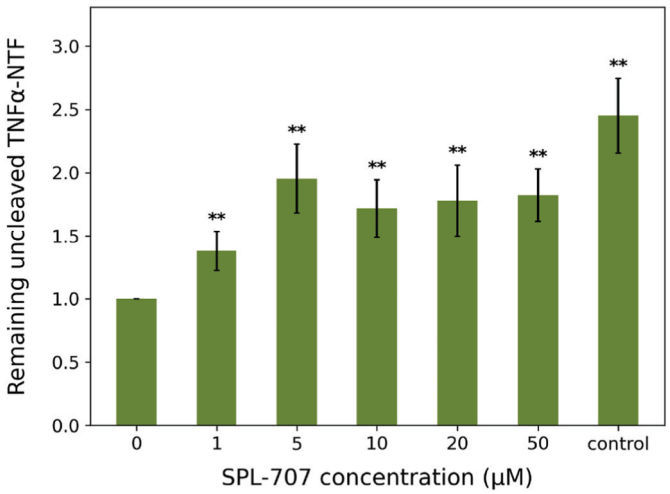

Fig. 6. Inhibition of SPPL2b in vitro activity by SPL-707 in a 96-well plate based set up. TNFα-NTF in vitro cleavage was carried out as described in Fig. 5 with addition of 0.02 % azide and 5 μM GI254023X. The total assay volume was reduced to 25 % of the original volume and incubation with FLAG-coupled magnetic beads was performed in a 96-well plate. SPPL2b was inhibited by SPL-707 at the indicated concentrations. After removal of the V5-tagged TNFα C-peptide the remaining TNFα-NTF was detected using an HRP-coupled *anti*-V5-antibody and the principle of a sandwich ELISA. Blank values comprising only buffer were subtracted and values were quantified relative to the amount of TNFα-NTF remaining after incubation without inhibitor. Note that the increase of the remaining TNFα-NTF corresponds to increased inhibition of SPPL2b activity. Mean ± SEM, Mann-Whitney *U* test for pairwise comparison between each of the groups and the control group without Inhibitor (0 μM). *, $p < 0.05$ relative to the respective samples without inhibitor. ($n = 8$). *, $p < 0.05$; **, $p < 0.01$.

5. Discussion

This study describes the development of the first in vitro assay for a member of the SPPL proteases based on separate isolation of the protease and the substrate. So far, substrate processing by SPPL proteases was mainly analyzed in intact cells or membranes [20,26,29,30,37,54–57]. This limited mechanistic analysis to enzyme and substrate variants that colocalize in the same subcellular compartments and are expressed in the same cell. Moreover, a yet to be discovered mechanism may involve complex spatial and temporal dynamics as well as changes in substrate concentration, co-factors, and chemical environment that in sum are difficult to decipher solely through in vivo studies. This might be the reason why the number of known SPPL substrates is very limited. Kinetic studies, to, for instance, determine whether intramembrane proteolysis by the SPP/SPPL family follows the rules of Michaelis-Menten-Kinetic, are only possible if the substrate concentration can be precisely titrated.

Over the past years, effort was put in transferring the well-established in vitro γ-secretase [31,33,34] and SPP [35,44] assays to SPPL proteases, however without success. We now developed conditions that allowed cleavage of TNFα-NTF isolated from one cell line by SPPL2b isolated from an independent cell line (Fig. 1), allowing their separate and localization independent combination as well as precise manipulation of experimental parameters. The following two fundamental changes of the assay conditions allowed in vitro cleavage of TNFα by SPPL2b. To increase an initially very faint signal, we isolated the substrate and its cleaved products utilizing anti-FLAG pull-down during incubation. The non-cleaved substrate as well as the cleavage products (TNFα-ICDs) were then clearly detectable on Western Blot and we observe various TNFα-ICD species, typical for the processive cleavages of SPPL2b on TNFα (Fig. 2A and [29,30]).

Second, it is well known that the lipid composition is crucial for the enzymatic activity of intramembrane proteases [49] and that lipid and detergent supplements are crucial for in vitro activity of γ-secretase [31,58–61] and SPP [23,44]. In contrast to γ-secretase, the detergent CHAPSO was used above its CMC to allow efficient SPPL2b in vitro activity. Thus, solubilization of protease and substrate in micelles seems to be important for SPPL2b in vitro activity. This is surprising as γ-secretase is reported to be inactive at CHAPSO concentrations above the CMC [31]. For SPP in vitro cleavage, a different detergent, N-Dodecyl-β-D-maltoside (DDM), is used at the same concentration (0.25 %) as CHAPSO in the established γ-secretase assays [44]. However, DDM has a very low CMC of 0.0087 % in water. Therefore, the requirement of a micelle forming condition might be a common feature for SPP/SPPL protease activity in vitro.

The substrate, TNFα-NTF, appears as multiple bands when visualized via the N-terminal FLAG-tag, but as a single band when visualized via the C-terminal V5-tag (Fig. 2B) independent of whether it is incubated with cell extracts lacking SPPL2a and SPPL2b (Fig. 2), containing the catalytically inactive SPPL2b variant (Fig. 3) or catalytically active SPPL2b (Fig. 2). It is likely, that this non-specific cleavage results from membrane associated proteases present in the assay and during substrate expression in the cell. Since cleavage of TNFα by, for instance, ADAM proteases is not restricted to the major cleavage site, which is depleted in the model substrate, it might well be that ADAM proteases contribute to this processing. However, also the presence of other unrelated exopeptidases cannot be excluded. Similar truncations of TNFα-NTF have also been observed earlier [30]. To overcome this, further purification of enzyme and substrate and/or sequence optimization of the model substrate will be required. However, since these are all membrane anchored proteins, purification and reconstitution in an active conformation turns out to be difficult.

In contrast to γ-secretase [31,59,60] changes in the PC concentration had no significant effect on the catalytic activity of SPPL2b in vitro (Fig. 2C). This difference might be attributed to the micelle condition, where the dynamics of lipid association to the protease will probably differ substantially from a non-micelle containing environment and, thus, the effects of other lipids might be masked.

Similar to γ-secretase, the cholesterol concentration significantly affected SPPL2b activity (Fig. 2D). However, we refrained from solubilizing cholesterol in chloroform and methanol to not harm our assay conditions but rather dissolved it directly in assay buffer. Despite this limitation in condition comparability, we observe the best cholesterol concentration in a similar range – 0.025 %–0.05 % as was reported to be optimal for γ-secretase [31]. In line with previous data, we observe protein aggregation effects at higher cholesterol concentrations [31]. This might be explained by limitations in solubility of cholesterol at the given conditions. Nonetheless, these data again highlight the importance of cholesterol for efficient intramembrane catalysis and demonstrate that the SPPL2b in vitro assay is sensitive to additive titration, and, thus, allows to study reaction conditions of SPPL2b in much more detail than before.

Activity assays based on co-expression of enzyme and substrate are also limited in comparing the catalytic activity of different enzyme variants, since similar expression levels of the different enzymes are hardly achieved without also affecting substrate levels. Independent isolation of substrate and enzyme, however, allows any adaption of enzyme amount without changing the substrate input. Based on this, we demonstrate that catalytically inactive SPPL2b present at similar or even slightly higher amounts then the corresponding wt protease does not result in detectable TNFα-ICD products (Fig. 3B). This shows that the mere presence of the enzyme – for example as a scaffold for other proteases – is not sufficient for SPPL2b dependent proteolysis and will allow to reliably quantify the catalytic capacity of different SPPL2b mutants to better understand substrate selection and the catalytic mechanism of this enzyme in future.

In the reversed version of the in vitro assay, we detected the C-peptide, which resembles the ICD-counterpart of the initial cleavage

(Figs. 1 and 3C). It was specifically generated in the presence SPPL2b wt but was absent when the substrate was incubated with extracts from cells lacking endogenous SPPL2a and SPPL2b (Fig. 3C). Faint background signals were almost completely abolished (Fig. 3C, longer exposure) by the addition of an inhibitor cocktail containing the matrix-metalloprotease inhibitor Batimastat, as well as the ADAM10 specific inhibitor GI254023X, and general protease inhibitors. This again hints to the previously described [30] non-specific or ADAM mediated processing of the model substrate.

Mass-spectrometric analysis of the in vitro generated TNFα-ICD species revealed the same cleavage sites (Fig. 4) that had been described earlier for cleavage of TNFα by SPPL2b in cellular context [26,30]. Regarding the relative intensity the longer TNFα-ICD species terminating at L39 and S34 were more prominent in the in vitro derived samples compared to the TNMFα-ICD species resulting from co-expression of substrate and enzyme (Fig. 4). While upon co-expression substrate and enzyme already interact in the living cell and substrate binding to the enzyme to some extend has already taken place before and during membrane isolation, in the in vitro setup this process only starts when substrate and enzyme are mixed. In addition, in vitro micelles are formed, and insertion of substrate and enzyme occurs randomly and only about 50 % of the molecules are expected to have the correct orientation towards each other. Thus, in vitro the consecutive turnover of longer to shorter TNFα-ICD species at a given incubation time is expected to be slower than in the co-expression setup. Although in smaller quantities than in the co-expression, we can still detect the shorter TNFα-ICD species, indicating that indeed SPPL2b in micelle-based assay conditions exhibits the same processivity to the TNFα TM domain as described in intact cell membranes.

The SPP specific inhibitor $(Z\text{-}LL)_2$-Ketone and the SPPL2a specific inhibitor SPL-707 are both known to also inhibit SPPL2b in vivo with an estimated IC_{50} of 2,1 μM and 0,47 μM, respectively [36,51]. So far, SPL-707 had only been characterized for inhibition of SPPL2b in a cellular nuclear translocation imaging assay called HCA (high content assay) which led to the estimation of the inhibition constant [36,52]. Utilizing our novel SPPL2b in vitro assay we carried out the first in vitro biochemical characterization of this inhibitor. We show inhibition at a similar range as in the HCA ([36,52]; Figs. 2 and 5) as well as an indication for blocking of the processive turnover of TNFα-NTF by SPPL2b (Fig. 5C). SPL-707 was designed based on the γ-secretase inhibitor LY-411,575 and is a peptidomimetic inhibitor [36]. Due to potential competition with the substrate and only a micromolar potency of SPL-707 on SPPL2b-inhibition, it is explainable that even at high inhibitor concentrations proteolysis is not fully blocked (Fig. 5C). Similar observations on SPPL2b processive cleavage have also been made upon treatment with $(Z\text{-}LL)_2$-Ketone [29] suggesting that currently available SPP/SPPL inhibitors are only moderately suitable for complete SPPL2b inhibition. Finally, we transferred the Western Blot-based assay set up to a 96-well plate-based read out and repeated the inhibitor studies with SPL-707. Similar to the Western Blot-based setup, we observe 50 % inhibition of SPPL2b in a concentration range which is well in line with the previously reported IC_{50} derived from the HCA [36], validating the concept of the high-throughput assay format.

Altogether, this shows that the in-vitro cleavage assay developed in this study fully resembles the catalytic activity and the mechanistic principles described for SPPL2b dependent processing of TNFα in cellular context. This assay will provide the basis for further in vitro studies on SPPL2b where in contrast to cellular systems defined manipulation of substrate, enzyme, and additive concentrations as well as of timing is possible. Thus, important enzyme kinetic parameters such as Km values but also pharmacologically important Kon, Koff values and residence time, that are key figures in drug development [53] as well as the mode of inhibition can be elucidated in the future, supporting drug discovery in this field. Rapid screening of large compound libraries to identify potential enzyme inhibitors or activators and allowing fast and efficient analysis of multiple enzyme and substrate mutants to pinpoint crucial residues involved will be supported by the high-throughput technique. An in vitro assay is essential to elucidate whether SPP/SPPL dependent catalysis within the membrane even follows a true Michaelis-Menten Kinetic or whether other kinetic rules apply to this intramembrane proteolysis. Such analysis requires the titration of substrate to a fixed amount of enzyme during a time frame where the reaction is in the linear phase of catalysis. To decipher the kinetic rules of SPPL2b catalysis the present assay will require further optimization such as knowledge on the exact concentration of a further purified substrate and determination of the linear reaction phase. For soluble enzymes this is rather straight forward but for intramembrane catalysis important information like the time required for the substrate to meet the enzyme in the detergent lipid mixture is missing. In the presented assay we have waived on further purification, since TNFα-NTF is aggregation prone, and we intended to ensure the correct folding of the substrate. As for the other members of the SPPL family, so far no in vitro cleavage assays are available and the SPP in vitro assay is only available in combination with a synthetically derived substrate peptide [23,44], our SPPL2b in vitro assay will also serve as an important basis for the development of further assays that will allow detailed studies of other SPP/SPPL family members as well as of different enzyme substrate combinations.

CRediT authorship contribution statement

Kinda Sharrouf: Visualization, Validation, Methodology, Investigation, Formal analysis, Data curation. **Christine Schlosser:** Investigation, Data curation. **Sandra Mildenberger:** Investigation. **Regina Fluhrer:** Writing – review & editing, Supervision, Project administration, Methodology, Funding acquisition, Conceptualization. **Sabine Hoeppner:** Writing – review & editing, Writing – original draft, Validation, Supervision, Project administration, Methodology, Investigation, Funding acquisition, Formal analysis, Conceptualization.

Declaration of competing interest

The authors declare that they have no known competing financial interests or personal relationships that could have appeared to influence the work reported in this paper.

Data availability

Data will be made available on request.

Acknowledgment

This work was supported by grants of the Deutsche Forschungsgemeinschaft to Regina Fluhrer (254872893/FL 635/2–3) and intramural funding of the Faculty of Medicine at the University of Augsburg to Sabine Hoeppner. We thank the ZfP (Protein analysis Unit, BMC, Munich) for access to mass spectrometry and their service.

Appendix A. Supplementary data

Supplementary data to this article can be found online at https://doi.org/10.1016/j.cbi.2024.111006.

References

[1] R. Fluhrer, C. Haass, Signal peptide peptidases and gamma-secretase: cousins of the same protease family? Neurodegener. Dis. 4 (2–3) (2007) 112–116.
[2] A.A. Papadopoulou, R. Fluhrer, Signaling functions of intramembrane aspartyl-proteases, Front. Cardiovasc. Med. 7 (2020) 591787.
[3] T. Mentrup, et al., Physiological functions of SPP/SPPL intramembrane proteases, Cell. Mol. Life Sci. 77 (15) (2020) 2959–2979.
[4] M.S. Brown, et al., Regulated intramembrane proteolysis: a control mechanism conserved from bacteria to humans, Cell 100 (4) (2000) 391–398.
[5] M.S. Wolfe, Intramembrane-cleaving proteases, J. Biol. Chem. 284 (21) (2009) 13969–13973.

[6] B. Brosig, D. Langosch, The dimerization motif of the glycophorin A transmembrane segment in membranes: importance of glycine residues, Protein Sci. 7 (4) (1998) 1052–1056.
[7] D. Langosch, et al., Understanding intramembrane proteolysis: from protein dynamics to reaction kinetics, Trends Biochem. Sci. 40 (6) (2015) 318–327.
[8] S.F. Lichtenthaler, M.K. Lemberg, R. Fluhrer, Proteolytic ectodomain shedding of membrane proteins in mammals-hardware, concepts, and recent developments, EMBO J. 37 (15) (2018).
[9] S.S. Yucel, M.K. Lemberg, Signal peptide peptidase-type proteases: versatile regulators with functions ranging from limited proteolysis to protein degradation, J. Mol. Biol. 432 (18) (2020) 5063–5078.
[10] C. Haass, H. Steiner, Alzheimer disease gamma-secretase: a complex story of GxGD-type presenilin proteases, Trends Cell Biol. 12 (12) (2002) 556–562.
[11] C. Haass, et al., Trafficking and proteolytic processing of APP, Cold Spring Harb. Perspect. Med. 2 (5) (2012) a006270.
[12] A.P. Grigorenko, et al., Novel class of polytopic proteins with domains associated with putative protease activity, Biochemistry (Mosc.) 67 (7) (2002) 826–835.
[13] C.P. Ponting, et al., Identification of a novel family of presenilin homologues, Hum. Mol. Genet. 11 (9) (2002) 1037–1044.
[14] A. Weihofen, et al., Identification of signal peptide peptidase, a presenilin-type aspartic protease, Science 296 (5576) (2002) 2215–2218.
[15] M. Voss, B. Schroder, R. Fluhrer, Mechanism, specificity, and physiology of signal peptide peptidase (SPP) and SPP-like proteases, Biochim. Biophys. Acta 1828 (12) (2013) 2828–2839.
[16] T. Mentrup, et al., The role of SPP/SPPL intramembrane proteases in membrane protein homeostasis, FEBS J 291 (1) (2023) 25–44.
[17] E. Friedmann, et al., SPPL2a and SPPL2b promote intramembrane proteolysis of TNFalpha in activated dendritic cells to trigger IL-12 production, Nat. Cell Biol. 8 (8) (2006) 843–848.
[18] J. Truberg, et al., Endogenous tagging reveals a mid-Golgi localization of the glycosyltransferase-cleaving intramembrane protease SPPL3, Biochim. Biophys. Acta Mol. Cell Res. 1869 (11) (2022) 119345.
[19] J. Schneppenheim, et al., The intramembrane proteases signal Peptide peptidase-like 2a and 2b have distinct functions in vivo, Mol. Cell Biol. 34 (8) (2014) 1398–1411.
[20] J. Niemeyer, et al., The intramembrane protease SPPL2c promotes male germ cell development by cleaving phospholamban, EMBO Rep. 20 (3) (2019).
[21] P. Krawitz, et al., Differential localization and identification of a critical aspartate suggest non-redundant proteolytic functions of the presenilin homologues SPPL2b and SPPL3, J. Biol. Chem. 280 (47) (2005) 39515–39523.
[22] S. Hoeppner, B. Schroder, R. Fluhrer, Structure and function of SPP/SPPL proteases: insights from biochemical evidence and predictive modeling, FEBS 290 (23) (2023) 5456–5474.
[23] S. Narayanan, T. Sato, M.S. Wolfe, A C-terminal region of signal peptide peptidase defines a functional domain for intramembrane aspartic protease catalysis, J. Biol. Chem. 282 (28) (2007) 20172–20179.
[24] G.M. McGeehan, et al., Regulation of tumour necrosis factor-alpha processing by a metalloproteinase inhibitor, Nature 370 (6490) (1994) 558–561.
[25] R.A. Black, et al., A metalloproteinase disintegrin that releases tumour-necrosis factor-alpha from cells, Nature 385 (6618) (1997) 729–733.
[26] R. Fluhrer, et al., A gamma-secretase-like intramembrane cleavage of TNFalpha by the GxGD aspartyl protease SPPL2b, Nat. Cell Biol. 8 (8) (2006) 894–896.
[27] K.M. Mohler, et al., Protection against a lethal dose of endotoxin by an inhibitor of tumour necrosis factor processing, Nature 370 (6486) (1994) 218–220.
[28] R.A. Black, et al., Relaxed specificity of matrix metalloproteinases (MMPS) and TIMP insensitivity of tumor necrosis factor-alpha (TNF-alpha) production suggest the major TNF-alpha converting enzyme is not an MMP, Biochem. Biophys. Res. Commun. 225 (2) (1996) 400–405.
[29] R. Fluhrer, et al., Intramembrane proteolysis of GXGD-type aspartyl proteases is slowed by a familial Alzheimer disease-like mutation, J. Biol. Chem. 283 (44) (2008) 30121–30128.
[30] C. Spitz, et al., Non-canonical shedding of TNFalpha by SPPL2a is determined by the conformational flexibility of its transmembrane helix, iScience 23 (12) (2020) 101775.
[31] P.C. Fraering, et al., Purification and characterization of the human gamma-secretase complex, Biochemistry 43 (30) (2004) 9774–9789.
[32] W.T. Kimberly, et al., Notch and the amyloid precursor protein are cleaved by similar gamma-secretase(s), Biochemistry 42 (1) (2003) 137–144.
[33] Y.M. Li, et al., Presenilin 1 is linked with γ-secretase activity in the detergent solubilized state, Proc. Natl. Acad. Sci. USA 97 (11) (2000) 6138–6143.
[34] D. Edbauer, et al., Reconstitution of gamma-secretase activity, Nat. Cell Biol. 5 (5) (2003) 486–488.
[35] A. Weihofen, et al., Release of signal peptide fragments into the cytosol requires cleavage in the transmembrane region by a protease activity that is specifically blocked by a novel cysteine protease inhibitor, J. Biol. Chem. 275 (40) (2000) 30951–30956.
[36] J. Velcicky, et al., Discovery of the first potent, selective, and orally bioavailable signal peptide peptidase-like 2a (SPPL2a) inhibitor displaying pronounced immunomodulatory effects in vivo, J. Med. Chem. 61 (3) (2018) 865–880.
[37] A.A. Papadopoulou, et al., Helical stability of the GnTV transmembrane domain impacts on SPPL3 dependent cleavage, Sci. Rep. 12 (1) (2022) 20987.
[38] Python Software Foundation, 2023, version 3.11.4. http://www.python.org4.
[39] Matplotlib Development Team, 2023, version 3.7.2. http://matplotlib.org.
[40] NumPy Contributors, 2023, version 1.25.1. http://numpy.org.
[41] SciPy developers, version 1.11.1, 2023. http://numpy.org.
[42] M.L. Moss, et al., Cloning of a disintegrin metalloproteinase that processes precursor tumour-necrosis factor-alpha, Nature 385 (6618) (1997) 733–736.
[43] A.M. Wang, et al., Molecular cloning of the complementary DNA for human tumor necrosis factor, Science 228 (4696) (1985) 149–154.
[44] T. Sato, et al., Signal peptide peptidase: biochemical properties and modulation by nonsteroidal antiinflammatory drugs, Biochemistry 45 (28) (2006) 8649–8656.
[45] D. Sjostrand, et al., A rapid expression and purification condition screening protocol for membrane protein structural biology, Protein Sci. 26 (8) (2017) 1653–1666.
[46] Y. He, K. Wang, N. Yan, The recombinant expression systems for structure determination of eukaryotic membrane proteins, Protein Cell 5 (9) (2014) 658–672.
[47] V. Rudajev, J. Novotny, Cholesterol-dependent amyloid beta production: space for multifarious interactions between amyloid precursor protein, secretases, and cholesterol, Cell Biosci. 13 (1) (2023) 171.
[48] M.S. Brown, J.L. Goldstein, The SREBP pathway: regulation of cholesterol metabolism by proteolysis of a membrane-bound transcription factor, Cell 89 (3) (1997) 331–340.
[49] S. Paschkowsky, F. Oestereich, L.M. Munter, Embedded in the membrane: how lipids confer activity and specificity to intramembrane proteases, J. Membr. Biol. 251 (3) (2018) 369–378.
[50] L. Martin, et al., Regulated intramembrane proteolysis of Bri2 (Itm2b) by ADAM10 and SPPL2a/SPPL2b, J. Biol. Chem. 283 (3) (2008) 1644–1652.
[51] Y. Ran, et al., Differential inhibition of signal peptide peptidase family members by established gamma-secretase inhibitors, PLoS One 10 (6) (2015) e0128619.
[52] X. Zhang, et al., Identification of SPPL2a inhibitors by multiparametric analysis of a high-content ultra-high-throughput screen, SLAS Discov. 22 (9) (2017) 1106–1119.
[53] K.E. Knockenhauer, R.A. Copeland, The importance of binding kinetics and drug-target residence time in pharmacology, Br. J. Pharmacol. (2023). https://doi.org/10.1111/bph.16104.
[54] M. Ballin, et al., The intramembrane proteases SPPL2a and SPPL2b regulate the homeostasis of selected SNARE proteins, FEBS J 290 (9) (2022) 2320–2337.
[55] A.A. Papadopoulou, et al., Signal Peptide Peptidase-Like 2c (SPPL2c) impairs vesicular transport and cleavage of SNARE proteins, EMBO Rep. 20 (3) (2019).
[56] M. Voss, et al., Foamy virus envelope protein is a substrate for signal peptide peptidase-like 3 (SPPL3), J. Biol. Chem. 287 (52) (2012) 43401–43409.
[57] M. Voss, et al., Shedding of glycan-modifying enzymes by signal peptide peptidase-like 3 (SPPL3) regulates cellular N-glycosylation, EMBO J 33 (24) (2014) 2890–2905.
[58] F. Kamp, et al., Intramembrane proteolysis of beta-amyloid precursor protein by gamma-secretase is an unusually slow process, Biophys. J. 108 (5) (2015) 1229–1237.
[59] P. Osenkowski, et al., Direct and potent regulation of gamma-secretase by its lipid microenvironment, J. Biol. Chem. 283 (33) (2008) 22529–22540.
[60] O. Holmes, et al., Effects of membrane lipids on the activity and processivity of purified gamma-secretase, Biochemistry 51 (17) (2012) 3565–3575.
[61] E. Dawkins, et al., Membrane lipid remodeling modulates gamma-secretase processivity, J. Biol. Chem. 299 (4) (2023) 103027.